Structural analysis and elastic characterization of air plasma sprayed ceria-yttria co-stabilized zirconia coatings

M. Alfano, L. Pagnotta, G. Stigliano
Department of Mechanical Engineering, University of Calabria
Via Ponte Pietro Bucci, Cubo 45C, 87036 Rende (CS) - ITALY
alfano@unical.it

G. Di Girolamo, C. Blasi
ENEA, CR Brindisi
S.S. Appia, km 713, 72100 Brindisi - ITALY
giovanni.digirolamo@brindisi.enea.it

Abstract: - The hot sections of gas turbine engines (*e.g.* blades, vanes, ducts, seals and airfoils) are usually exposed to extremely hot gases which coupled to the action of oxidative and corrosive environments provide the ideal conditions for nucleation and growth of cracks. It follows that the surface temperature of these components must be maintained low enough to retain materials properties within acceptable bounds and to extend component life. From this standpoint, the most promising approach is represented by the application of ceramic thermal insulating layer which shields the substrate from the hot gas heat source. To this purpose, Air Plasma Sprayed (APS) yttria stabilized zirconia (YSZ) has been often adopted in the last decades. However, the main drawback of YSZ is represented by the phase stability at higher temperature. For this reason new alternative materials have been proposed. In particular, it has been observed that the addition of ceria to tetragonal zirconia allows to obtain ceria and yttria co-stabilized zirconia (CYSZ) which presents a higher phase stability than YSZ. The aim of the present work is the structural and elastic characterization of APS CYSZ coatings. In particular, X-Ray diffraction was used for phase analyses while the morphology and the final microstructure of the coatings were analyzed by SEM investigations. In addition, the stiffness (i.e. Young's modulus) of CYSZ is measured by means of a resonant method applied to beam-like coated samples.

Key-Words: - Thermal barrier coatings, ceria-yttria stabilized zirconia, Young's modulus, impulse excitation technique

1 Introduction

Nickel and cobalt based superalloys are widely used in stationary turbines of power plants and aircraft engines because of their capability to withstand high temperature without exhibiting degradation mechanisms (e.g. melting, creep, oxidation, thermal fatigue, etc). To this aim the maximum operating temperature of these alloys has continually been enhanced (>1000^{o}C) by means of composition refinement, directional grain growth or single crystal alloy development [1]. However, surface material is exposed to extremely hot gases which coupled to the action of oxidative and corrosive environment provide the ideal conditions for nucleation and growth of cracks. It follows that the surface temperature must be maintained low enough to retain materials properties within acceptable bounds and to extend component life. From this standpoint, the most promising approach consists in placing a thermal insulating layer of material, namely a Thermal Barrier Coating (TBC), on the surface of blades, vanes, ducts, seals and airfoils in the hot sections of gas turbine engines. Such TBCs, applied in the form of thin films typically measuring less than a millimeter, allow for a reduction in heat transfer to the underlying components [2-5].

Typically, a TBC system consist of a bond coat and a top coat. The bond coat is a metallic layer which provides oxidation protection to the substrate and a suitable surface onto which the top coat adheres. The top coat is a ceramic layer whose composition is selected based on thermal conductivity, high temperature stability and thermal expansion compatibility with the substrate.

Various techniques have been developed for coating deposition, one of the most widespread is the Air Plasma Spray (APS) process. With such a technology, a gas streaming in a burner through an high energy electric arc is transformed into an high temperature plasma. The individual components of the TBC are thus fed into the burner in the form of powder and are melted and driven by the plasma gas

to impact with high velocity on the substrate. The rapid solidification of impacted molten droplets give rise to a highly heterogeneous microstructure consisting of irregular thin lamellae known as 'splats'. The material mostly used for APS TBCs production purpose is yttria-stabilized zirconia (YSZ) because of its low thermal conductivity, good thermo-cyclic durability and phase stability. However, the drawback of YSZ is the tetragonal to martensitic (t→m) transformation occurring at high temperature which induces a disastrous volume expansion (from 3 to 5%) and coating fracture. In order to tackle this problem new alternative material have been proposed. In particular, it has been observed that the addition of ceria to tetragonal zirconia allows to obtain ceria and yttria co-stabilized zirconia (CYSZ) which presents an higher phase stability than YSZ and is particularly promising for technical demanding applications.
The aim of the present work is the structural and elastic characterization of APS CYSZ coatings. In particular, X-Ray diffraction was used for phase analyses while the morphology and the final microstructure of the coatings were analyzed by SEM and EDS investigations. In addition, the elastic modulus of CYSZ plasma spray deposits is also reported. To this aim, a procedure based on the measurement of the fundamental natural frequency of vibration of beam-like coated samples is adopted. An experimental apparatus for measuring the resonant frequencies is proposed where samples are excited to vibrate by impact and a microphone is used as receiver.

2 Microstructural analysis

2.1 Substrates preparation and plasma spraying

Plasma spraying was carried out using a Sulzer Metco APS system, equipped with a F4-MB plasma torch (Sulzer Metco AG, Switzerland) mounted on an industrial robot. The feedstock was the commercial Metco 205NS (ZrO_2-25CeO_2-2.5Y_2O_3) [6]. Stainless steel plates (310S) (25 mm x 25 mm x 4 mm dimensions) and Inconel superalloy (IN738) disks (25 mm diameter x 5 mm thickness) were used as substrates. Before spraying, the substrates were cleaned and degreased ultrasonically in ethanol and grit-blasted with alumina abrasive, to increase the roughness of their surface and consequently to improve the adhesion of the coatings on substrates. The spray parameters used during the depositions are summarized in Table 1. The resulting coatings show a thickness ranging between 400 and 450 μm. Before CYSZ deposition, a bond coat was applied in order to reduce thermal expansion mismatch between the substrate and the TBC and to enhance the adhesion of the same TBC. The powder used as bond coat was a commercial CoNiCrAlY (Amdry 995C) [6] and the thickness was about 100 μm.

Table 1 – Torch parameters used for Plasma Spraying the CYSZ powder.

Current (A)	600
Turntable velocity (rad/s)	100
Gun velocity (mm/s)	4
Powder carrier gas Ar (nlpm)	2.6
Primary gas Ar (nlpm)	38
Secondary gas H_2 (nlpm)	11
Stand off distance (mm)	120
Powder feed rate (g/min)	44.1

2.2 Phase analysis

The phase analysis and crystalline structures of the powder and coatings were investigated using an X-Ray diffractometer (XRD, Powder Diffractometer Philips PW1880), operating with CuKα (λ=0.154186 nm) radiation. The range analyzed of the diffraction angle (2θ) was between 20° and 80°, by step of 0.01°. X-Ray diffraction patterns of the powder and as-sprayed coating are shown in Fig. 1.

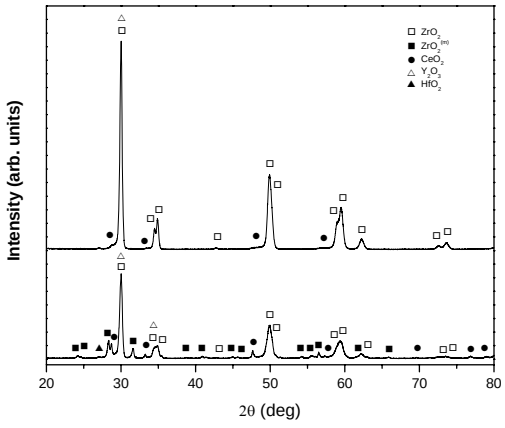

Fig. 1 - XRD patterns of CYSZ powder and as-sprayed coatings.

It can be seen that in the powder there was the tetragonal and a small amount of monoclinic phase of zirconia. After plasma spraying this last was not detected. Some peaks of the oxide stabilizers (CeO_2 and Y_2O_3) are clearly visible but, as expected, their intensities were reduced after plasma spraying, especially for CeO_2. This could mean a weight loss of this stabilizer which was evaporated in the

plasma plume. This fact should lead to a stoichiometry change and a partial reduction of the thermo-mechanical properties of the coating, when compared to bulk material having the same chemical composition (ZrO_2-$25CeO_2$-$2.5Y_2O_3$). So that, the main phase into the final coatings was non-transformable tetragonal t', due to rapid cooling rates during the plasma spray process. Really, there are two types of this tetragonal phase, such as a high stabilizer non-transformable tetragonal t' phase and a low stabilizer transformable tetragonal phase. In cooling to room temperature, the high stabilizer cubic phase may be retained or it may transform to a high stabilizer tetragonal phase. The low stabilizer tetragonal phase may transform to monoclinic. From the viewpoint of phase equilibrium, it can be concluded that CeO_2 provides a good partial stabilization of ZrO_2. So, it would be required a higher temperature and more time to allow the detrimental monoclinic transformation.

2.3 Microstructure

The morphology of starting powder as well as the microstructure of the as-sprayed coatings were analyzed by scanning electron microscopy (SEM, Philips XL40) with Energy Dispersive Spectrometer (EDS). The powder particles were spherical and showed a controlled, uniform particle size distribution, with dimensions ranging from 10 to 110 μm. These particles have been sintered and agglomerated into granules with spray drying by the manufacturer. As shown in Fig. 2, some of them, within the agglomerates, were nanosized, even if the powder agglomerates were microsized.

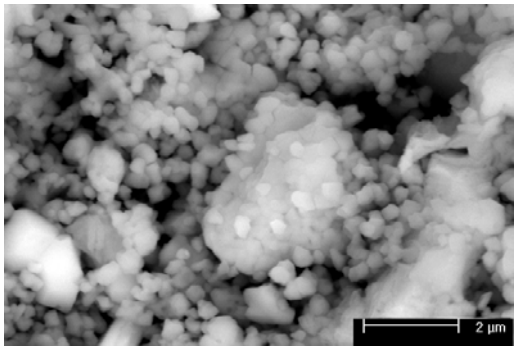

Fig. 2 - Morphology of nanosized particles into CYSZ agglomerated.

In order to analyze the microstructure of the coatings, metallographic surfaces and cross-sections were prepared using standard metallographic procedures. The specimens were cut with a low velocity diamond saw and then mounted in vacuum with an epoxy resin and finally polished until 1 μm.

Fig. 3 shows the cross-sectional microstructure of the entire TBC. As shown, an excellent adhesion existed between the top coat and the bond coat and between the bond coat and the substrate. In particular, the adhesion between the top coat and the bond coat is an important factor, since their relative thermal expansion coefficients are quite different and the failure of a TBC usually can be related to the formation of thermally grown oxide (TGO) on the bond coat surface and to the subsequent spallation of the ceramic coating. Anyway, the adhesion is improved by roughness of the interface between bond and top coat, which is higher than that of the grit-blasted substrate.

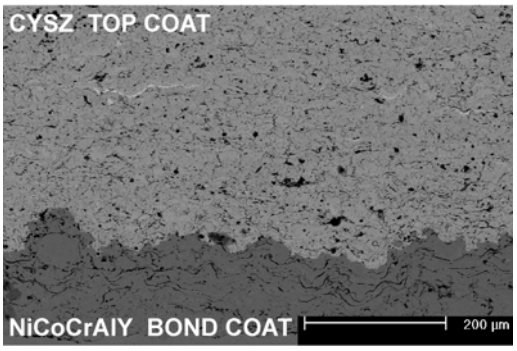

Fig. 3 - SEM micrograph of CYSZ TBC on IN738 substrate.

Fig. 4 shows more in details the complex microstructure of the ceramic coating.

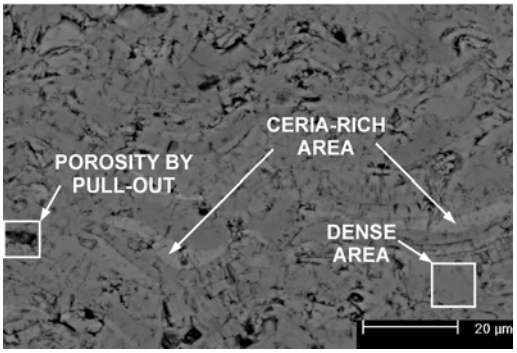

Fig. 4 – The typical porous-lamellar structure of CYSZ coatings.

As it can be seen, the coatings deposited by APS are characterized by a highly heterogeneous microstructure where the lamellae, or microsplats, are embedded in a network of microcracks and voids, and are able to slide past each other. Microcracks and pores play an important role for the high temperature properties, quality and thermal shock resistance, as effective paths for the salt in hot corrosion [7-9]. Different regions characterized by different grey contrasts can also be observed. This indicates elements and compounds with different atomic weight. In particular, because of the higher

scattering intensity of heavier atoms, the darker regions correspond to elements with lower atomic weight and the brighter regions to elements with higher atomic weight. EDS analysis demonstrated that the brighter areas were more rich of CeO_2 stabilizer than the others. So that in these zone the amount of non-transformable t' was expected to be higher. These areas are clearly observed in Fig. 4 and 5. Some dense areas are visible within the lamellae and they can be related to the good melting of the CYSZ powder particles, a signal of the high quality of the coatings. As shown in Fig. 5, looking more in deep the microstructure, it is possible to distinguish intersplat and intrasplat microcracks. The former are represented by cracks that run across the splat interfaces whereas the latter run across the splats. These cracks provide a reduction of thermal conductivity and an increase in thermal shock resistance. Nevertheless, their presence allows the corrosive agents to enter the coatings and deteriorate the TBC leading to its debonding or spallation.

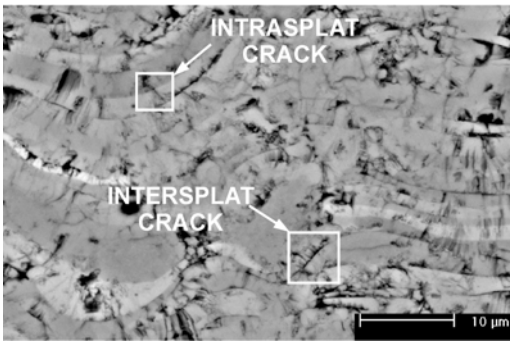

Fig. 5 – A view of common microcracks within the lamellar structure of CYSZ coatings.

The porosity fraction was estimated from SEM micrographs of the cross-section using a software suited for image analysis, namely ImageJ [10]. In particular, ten measures were performed for each cross-section. The image analysis allows to distinguish the pores which appears very dark and, subsequently, to evaluate the porosity level from a computation of pixels showing grey level variations. This technique permits to measure accurately the large pores, while the contribution of small pores and microcracks is more difficult to quantify. The average of porosity fraction for CYSZ coatings was about 9%, that is consistent with the typical values reported in literature for thermal sprayed ceramic coatings. From micrographs observation it can be assumed the typical bimodal distribution of porosity reported in literature, with large pores and fine pores, homogeneously distributed. The fine pores derive by gas entrapped under the liquid droplets, while the coarse pores can be associated with filling defects in the coating structure, caused by unmelted or semi-molten particles. An increase in porosity could also be attributed to the unavoidable pull-out phenomenon which occurs during polishing of cross-sections. The largest pores, of both circular and elongated shapes, showed in the micrographs can be attributed to this phenomenon. Even if these last are not equally distributed, they could cause systematic errors during measurements.

3 Elastic Characterization

3.1 Selection of the test methodology

As a results of the deposition process, the coatings present properties quite different from the corresponding bulk materials of the same composition. Indeed, unlike dense ceramics, the final microstructure of plasma sprayed deposits is characterized by the presence of cracks. These last have a severe impact on the mechanical properties as they induce an anisotropic behaviour. In particular, inter-lamellar cracks and pores affect the in-plane elastic modulus, whereas the out of plane elastic modulus is affected by the intra-lamellar cracks [11,12]. As a consequence, it is necessary to consider the measurement direction in determining the elastic modulus of the deposit or comparing the results of different techniques.

For instance, it has been demonstrated in [12] that the elastic modulus of the APS coatings determined by Nano-Indentation (NI) is different with respect to Bending Test (BT).

BT works at the macroscopic level and provides the in-plane elastic modulus as the tangent of the stress-strain curve of the coating. Owing to splat boundary sliding and propagation of cracks, inelastic deformations occur during testing and, as a consequence, the results of BTs are affected by this non linear stress-strain behavior.

NI probes the microstructure at the splat level, *i.e.* the microscopic scale, and, owing to the limited test volume, the resulting out of plane elastic modulus is nearly that of the splat itself. Therefore it is different with respect to that of BT (usually higher) and this effect is more pronounced in ceramics than in metals coatings [13,14].

Even if NI and BT are currently used in order to obtain the elastic properties of plasma deposits [15,16], they are too tedious for a routine and cost-effective application in production. As an alternative, the use of dynamic test methods, in particular the resonant methods, has increased in the last decades [17-20]. They allow to determine the elastic modulus if a suitable equation, namely the frequency equation, relating the natural frequencies,

the mass and geometrical properties of the specimens is known.
To this aim it is necessary to measure the resonant frequencies of the specimen. From this standpoint sample vibration, in the sonic and/or ultrasonic range, is achieved by continuous variable excitation, generally of sinusoidal or random stationary type, or by impact. With the latter technique, often mentioned as the Impulse Excitation Technique (IET), oscillations are induced in the sample by a single mechanical impact and the resulting transient signal is detected by a microphone and digitally analyzed in order to extract the resonant frequencies. IET has the advantage of being simple, fast and accurate and requires inexpensive experimental equipment and can certainly be used for rapid production process monitoring. In addition, IET allows to determine the elastic moduli subjecting the specimen to lower strains so that they are measured nearly at the origin of the stress-strain curve, thus fracture and non linear material response are then prevented.

3.2 Theoretical background

The frequency equation, can generally be obtained integrating the equation of motion in accordance with the prescribed boundary conditions. For example, an exact solution of the three dimensional form of the differential equation of motion was obtained for the axial and the torsional vibrations of an infinite length isotropic circular bar with free edge conditions. For finite length isotropic bars (circular or rectangular cross sections) and other simple geometries, such as circular thick plates, only approximate numerical solutions exist and these approximate numerical solutions are recommended in ASTM standards for the elastic characterization of isotropic materials [17]. Nevertheless, different geometries could also be used if the corresponding frequency equations are known. For example, a procedure that extends resonant method to isotropic samples in the form of thin rectangular plates was proposed in [18] and subsequently it was applied to a free standing diamond coating in [19,20]. However, the methodologies mentioned above are not suited for coated samples (*i.e.* coating/substrate system), like those analyzed in this paper. Therefore, it is necessary to develop a proper frequency equation. To this aim, let consider a composite beam consisting of two homogeneous, isotropic, linear elastic layers with constant cross sections. Neglecting shear and rotary inertia effect, and assuming a perfect bonding at the interface the transverse (i.e. flexural) vibration are described by the following well known Bernoulli-Euler equation

$$-\left(E_c I_c + E_s I_s\right)\frac{\partial^4 w}{\partial x^4} = \left(\rho_c A_c + \rho_s A_s\right)\frac{\partial^2 w}{\partial t^2} \qquad (1)$$

where I is the moment of inertia about the centroidal axis of the beam, w(x,t) is the transverse displacement, A is the cross sectional area, ρ is the mass density, E is the modulus of elasticity while the subscripts c and s denote the coating and the substrate, respectively. A schematic depiction of the resulting composite beam is reported in Fig. 7.

Fig. 7 – Schematic representation of a bi-material beam.

In order to solve Eq. 1, one can resort to the method of separation of variables. Therefore, considering harmonic free vibrations, the transverse displacements can be written as

$$w(x,t) = W(x)\, e^{i\omega t} \qquad (2)$$

where ω is the frequency of vibration and W(x) is a mode shape function. Substitution of this solution in Eq. (1) and rearranging yields the following

$$\frac{d^4 W(x)}{dx^4} - k^4\, W(x) = 0 \qquad (3)$$

where

$$k = \left[\frac{\rho_c A_c + \rho_s A_s}{E_c I_c + E_s I_s}\omega^2\right]^{1/4} \qquad (4)$$

A suitable shape function for solving Eq. 3 has the following form

$$W(x) = C_1 \sin(kx) + C_2 \cos(kx) + \\ + C_3 \sinh(kx) + C_4 \cosh(kx) \qquad (5)$$

where the C_i are integer constants which depend on the boundary conditions. From the experimentalist point of view it is advisable to choose free ends condition, because it is easier to reproduce and affects less frequency measurements if compared, for instance, with clamped configuration. As a consequence, for a free-free beam, since the bending moments and the shear forces are zero at both free ends, the boundary conditions of the transverse vibration are given by $W_{,xx}=0$, $W_{,xxx}=0$ at both x=0 and x=L. Imposing the boundary conditions it is possible to obtain $C_1=C_3$ and $C_2=C_4$. The remaining

equations give rise to system which solved for non-trivial solutions of C_1 and C_2 leads to the eigenvalue equation for the undamped free flexural vibration of a composite beam with free ends

$$\cos(k\,L)\cdot\cosh(k\,L)-1=0 \qquad (6)$$

It has an infinite number of solutions k_nL, where the subscript n refers to the mode number. The eigenvalues corresponding to the first four modes of vibration are easily found using the software package Mathematica (Wolfram, 2006) [21]. In particular, $k_1L=4.73004$, $k_2L=7.8532$, $k_3L=10.9956$ and $k_4L=14.1372$. Substituting the eigenvalues in the definition of k, i.e. Eq. (4), and using the relationship $\omega=2\pi f$, it is possible to obtain the frequency equation

$$f_n=\frac{(k_nL)^2}{2\pi L^2}\left(\frac{E_cI_c+E_sI_s}{\rho_cA_c+\rho_sA_s}\right)^{1/2} \qquad (7)$$

The in-plane elastic modulus of the coating can thus be obtained using the above Eq. 7. As it is in implicit form an iterative procedure should be used. However, in this work the software package Mathematica will be adopted.

3.2 Experimental procedures

For mechanical properties investigation, stainless steel plates (100 mm x 25 mm x 4 mm) were used as substrates and coated with CYSZ. In order to simplify the identification procedure, the bond coat was not applied. Nevertheless, the adhesion between coating and substrate was excellent. Other authors showed that the elastic modulus of the coating does not depend on coating thickness [22]. For each specimen a deposit thickness approximately equal to 350 μm was chosen. So, the tests were carried out on nominally identical coated samples whose dimensions are reported in Table 2. Thickness measurement is always critical for the quality of the results therefore a digital micrometer with a resolution of one-thousandth of a millimeter was used. For all the other length measurements a standard caliper with a resolution of one-fiftieth of a millimeter was used. The mass density of the steel substrates has been determined from the plate volume and mass. This last has been measured by a precision digital balance which is accurate to one-hundredth of a gram. The value obtained for the substrates is 7.78 g/cm^3. The mass density of the coating is that specified by the manufacturer, *i.e.* 5.4 g/cm^3 [6].

Table 2 - Samples dimensions (mm)

		P1		P2		P3	
	dof	$\bar{x}$	$u(\bar{x})$	$\bar{x}$	$u(\bar{x})$	$\bar{x}$	$u(\bar{x})$
length, L	2	100.53	0.01	100.55	0.05	99.73	0.03
width, B	4	25.08	0.02	25.09	0.01	24.92	0.01
thickness, t_s	5	3.986	0.012	4.021	0.004	4.027	0.003
thickness, t_c	5	0.362	0.017	0.357	0.019	0.367	0.014

$\bar{x}$: mean value of n measurements;
$u(\bar{x})$: standard uncertainty [23];
d.o.f.= n-1: degree of freedom;

Before plasma spraying the elastic properties of the substrates were determined following the procedures and the recommendation of the ASTM standards for the elastic characterization of isotropic materials [14]. Subsequently, the Young modulus of the deposit has been determined using Eq. 1. In both case the measurement of the fundamental natural frequency is needed. From this standpoint, specimens suspension is of critical concern in order to achieve good quality frequency measurement. The procedure adopted herein requires specimens with all the edges free in order to accommodate the boundary conditions prescribed from Eq. 1. Therefore, each samples were supported on direct contact supports made of soft material (*e.g.*, cotton pad, soft sponge) showing a minimal contact area with the specimen. They were placed in locations that allow the plate to oscillate without significant limitation in the desired mode (see Fig. 3). Impact excitation was imparted lightly hitting the beam and the resulting vibration was picked up using a microphone (Trust MC200, frequency bandwidth from 50Hz to 14000 Hz) placed near the surface of the sample under examination. The dynamic response detected by the microphone was then analyzed and processed by a suitable program written in MATLAB^{TM} [24] environment. It transforms the sampled time functions into a frequency spectrum by a Fast Fourier Transform (FFT) algorithm allowing the identification of the fundamental natural frequency. The resolution of the measurement system depends on the time length (t_a) of the signal acquired. In this work, each measurement was carried out using an acquisition time equal to 10s. Using a sampling frequency of 44100Hz a resolution equal to $\Delta f = 1/\Delta t = 0.1$ Hz is achieved. No significant deviation were observed among the values of repeated measurements. In order to mitigate the environmental noise and to better illustrate the peaks of the frequency spectrum,

the average signal obtained by impacting the plate three times has been analyzed.

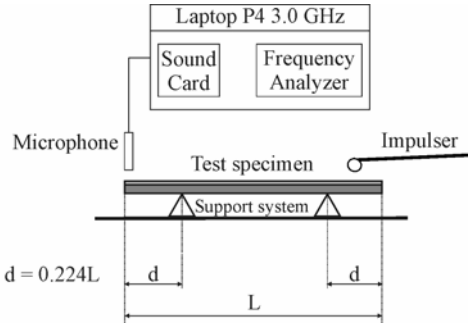

Fig. 8 - Block diagram of the test set-up

3.3 Results and discussion

The results obtained for the elastic modulus are reported in this section. In particular Table 3, reports the fundamental natural frequency of the substrate before coating deposition.

Table 3 - Fundamental natural frequency and Young's modulus of the steel substrates

	f_{1s} [Hz]	E_s [GPa]		
		$\bar{x}$	$u(\bar{x})$	$U(\bar{x})$ (95%)
P1	2104.5	212.13	1.90	4.87
P2	2107.1	208.92	0.70	1.71
P3	2148.9	209.95	0.51	1.24

U(x): combined standard uncertainty (coverage factor k=t_{95}, t is the t-student distribution) [23]

This last together with the geometrical dimension and the mass density of the substrate material (see Table 2) allows to determine the Young modulus following the procedure and the recommendations reported in the ASTM Standard test methods [17]. The results present a reduced scatter and are in agreement with the common values reported for steel. The elastic modulus of the coatings are reported in Table 4.

Table 4 - Fundamental natural frequency and Young's modulus of the CYSZ coating

	f_{1sc} [Hz]	E_c [GPa]		
		$\bar{x}$	$u(\bar{x})$	$U(\bar{x})$ (95%)
P1	2092.0	25.10	4.53	11.09
P2	2094.7	25.50	2.20	4.50
P3	2134.1	23.41	1.52	3.14

U(x): combined standard uncertainty (coverage factor k= t_{95}, t is the t-student distribution) [23]

In particular, Table 4 presents the fundamental frequency of the coated samples, which introduced in Eq. 1 and considering the geometrical and mass properties reported in Table 2, allows to obtain the elastic modulus of the coating. The values obtained are characterized by relatively large scatter, however, they are in agreement with those reported in the literature [24,25].

4 Conclusion and perspectives

In this paper, the microstructure and the elastic modulus of an Air Plasma Sprayed Ceria-Yttria co-stabilized zirconia coating has been analyzed. In particular, XRD spectra showed that the main phase in the coating was tetragonal zirconia while SEM analyses revealed a lamellar microstructure characterized by the presence of intra-lamellar and inter-lamellar cracks and pores. The elastic characterization has been carried out using the IET. It has the advantage of being simple, fast and accurate, furthermore, it requires inexpensive experimental equipment and can certainly be used for rapid production process monitoring. Furthermore, the results obtained are in good agreement with those reported in literature.

Anyhow, it is worth noting, that the applicability of the procedure proposed herein requires the stress state in the beam to be truly uniaxial. Therefore the specimen must be very narrow so that no appreciable stress can develop in the transversal direction. This means that the width of the bi-layer specimen should not be much larger than the thickness of the coating. However, this condition can hardly be satisfied, especially in specimen with very thin coatings, therefore for such cases alternative methodologies should be adopted. For this reason, the authors are currently developing an alternative procedure based on 3D-Finite Element Models of the test beams.

Acknowledgmentes

L. Capodieci for SEM observation and T. Nocco for XRD measurements.

References:

[1] J. Mencik, *Mechanics of components with treated or coated surfaces*, Kluwer Academic Publishers Group, 1996.

[2] J. A. Nesbitt, Thermal response of various thermal barrier coatings in a high heat flux rocket engine, *Surface and Coatings Technology*, Vol. 43-44, No. 1, 1990, pp. 458-469.

[3] T. M. Yonushonis, Overview of thermal barrier coatings in diesel engines, *Journal of Thermal Spray Technology*, Vol. 6, No. 1, 1997, pp. 50-56.

[4] R. A. Miller, Current status of thermal barrier coatings - An overview, *Surface and Coatings Technology*, Vol. 30, No. 1, 1987, pp. 1-11.

[5] Y. Li and K. A. Khor, Mechanical properties of the plasma-sprayed Al2O3/ZrSiO4 coatings, *Surface and Coatings Technology*, Vol. 150, No. 2-3, 2002, pp. 143-150.

[6] www.sulzermetco.com

[7] S. Y. Park, J. H. Kim, M. C. Kim, H. S. Song and C. G. Park, Microscopic observation of degradation behavior in yttria and ceria stabilized zirconia thermal barrier coatings under hot corrosion, *Surface and Coatings Technology*, Vol. 190, No. 2-3, 2005, pp. 357-365.

[8] X. Q. Cao, R. Vassen and D. Stoever, Ceramic materials for thermal barrier coatings, *Journal of the European Ceramic Society*, Vol. 24, No. 1, 2004, pp. 1-10.

[9] R.Vassen, F.Tietz, G.Kerkhoff and D.Stoever: in Proceedings of the 6th Liége Conference on Materials for Advanced Power Engineering, *eds. J. Lecomte Beckers, F.Schuber and P. J. Ennis*, Forschungszentrum Juelich GmbH, Juelich Deutschland, 1998, 1627.

[10] http://rsb.info.nih.gov/ij

[11] B. Siebert, C. Funke, R. Vaβen and D. Stöver, Changes in porosity and Young's Modulus due to sintering of plasma sprayed thermal barrier coatings, *Journal of Materials Processing Technology*, Vol. 92-93, No. 1999, pp. 217-223.

[12] H. J. Kim and Y. G. Kweon, Elastic modulus of plasma-sprayed coatings determined by indentation and bend tests, *Thin Solid Films*, Vol. 342, No. 1-2, 1999, pp. 201-206.

[13] S.Y. Park, J.H. Kim, M.C. Kim, H.S. Song, C.G. Park, Microscopic observation of degradation behaviour in yttria and ceria stabilized zirconia thermal barrier coatings under hot corrosion, *Surf. Coat. Technol.* Vol. 190, pp. 357-365, 2005.

[14] F. Kroupa and J. Plesek, Nonlinear elastic behavior in compression of thermally sprayed materials, *Materials Science and Engineering: A*, Vol. 328, No. 1-2, 2002, pp. 1-7.

[15] M. Beghini, L. Bertini and F. Frendo, Measurement of coatings' elastic properties by mechanical methods: Part 1. Consideration on experimental errors, *Experimental Mechanics*, Vol. 41, No. 4, 2001, pp. 293-304.

[16] M. Beghini, G. Benamati, L. Bertini and F. Frendo, Measurement of coatings' elastic properties by mechanical methods: Part 2. Application to thermal barrier coatings *Experimental Mechanics*, Vol. 41, No. 4, 2001, pp. 305-311.

[17] L. Pagnotta, G. Stigliano, A numerical-experimental approach for identification of material constants of composite laminates by displacement field measurement, WSEAS Transactions on Applied and Theoretical Mechanics, 1 (1), (2006) 39 – 46.

[18] M. Alfano and L. Pagnotta, Determining the elastic constants of isotropic materials by modal vibration testing of rectangular thin plates, *Journal of Sound and Vibration*, Vol. 293, No. 1-2, 2006, pp. 426-439.

[19] M. Alfano and L. Pagnotta, Measurement of the dynamic elastic properties of a thin coating, *Review of Scientific Instruments*, Vol. 77, No. 5, 2006, pp. 056107-3.

[20] M. Alfano and L. Pagnotta, A non destructive technique for the elastic characterization of thin isotropic plates, *NDT&E International*, Vol. 40, No. 2, 2007, pp. 112-120.

[21] Stephen Wolfram, *the Mathematica Book, 4th ed.* (Wolfram Media/Cambridge University Press, 1999)

[22] T. Lauwagie, PhD dissertation, Vibration-based methods for the identification of the elastic properties of layered materials, Katholieke Universiteit Leuven, 2005

[23] Guide to Expression of Uncertainty in Measurement, *ISO*, Switzerland, 1995.

[24] Matlab, The Mathworks inc., 1994-2007.

[25] T. Lauwagie, K. Lambrinou, S. Patsias, W. Heylen, J. Vleugels Resonant-based identification of the elastic properties of layered materials: Application to air-plasma sprayed thermal barrier coatings, *NDT & E International*, Vol. 41, No. 2, 2008, pp. 88-97.